Journal of Organometallic Chemistry 696 (2011) 2429–2437

Contents lists available at ScienceDirect

Journal of Organometallic Chemistry

journal homepage: www.elsevier.com/locate/jorganchem

Phase behavior of some mono-substituted ferrocene- and [3] ferrocenophane-containing nematics with the cyclohexane ring in the rigid core

So Yeon Kim [a], Oleg N. Kadkin [a,b,*], Eun Ho Kim [a], Moon-Gun Choi [a,**]

[a] Department of Chemistry, Yonsei University, 262 Seongsanno, Seodaemun-Gu, Seoul 120-749, Republic of Korea
[b] Department of Physical and Colloid Chemistry, Kazan State Technological University, 68, K. Marks Str., 420015 Kazan, Russia

ARTICLE INFO

Article history:
Received 28 January 2011
Received in revised form
27 February 2011
Accepted 7 March 2011

Keywords:
Liquid crystals
Metallomesogens
Synthesis design
Phase transitions
Mesophases
Ferrocene

ABSTRACT

Generally, incorporation of the cyclohexane rings into the rigid core of rod-like mesogens leads to improved technological parameters, i.e. low viscosity, ambient transition temperatures and stability of the nematic state. Taking this into consideration, a series of novel cyclohexane-containing derivatives of ferrocene has been synthesized. The effect of various structural factors on liquid crystalline behavior of the synthesized ferrocene-containing nematics has been examined. Ferrocenophane compounds exhibited enhanced liquid crystalline properties in comparison with the derivatives of unbridged ferrocene. Depending on thermal prehistory of the samples, some of the synthesized ferrocenomesogens showed remarkable migration of the phase transition temperatures. In one case such behavior led to stabilization of the initially monotropic nematic mesophase in subsequent heating cycles. In another case, the phase transition shifts caused the lowering of the crystal-to-nematic transition temperature and the broadening of the mesophase range. There was also a case of alteration from the initially enantiotropic to monotropic behavior. The obtained novel metallomesogens are important footsteps toward the development of low-viscous and low-temperature materials for liquid crystal applications possessing a chromophoric, redox-switchable, polarizable and chemically stable superaromatic ferrocene unit.

1. Introduction

The presence of transition metals brings unusual properties to liquid crystals and opens wide possibilities for new applications. This perception stimulated A.M. Giroud-Godquin and others to start systematic studies of metal-containing liquid crystals in 1977 [1,2]. Ferrocene-containing liquid crystals among various types of metallomesogenic systems attracted reasonable interest of researchers during recent decades [3,4]. Certainly, a chemical and thermal stability of superaromatic ferrocene moiety radically exceeds a stability of other metal-containing coordination sites that are traditionally used in the molecular design of metallomesogens. Besides, ferrocene is a good chromophore, redox-switchable and polarizable unit due to the increased electronic density around the metal center. Hence, mesogenic ferrocene derivatives are valuable candidates for potential applications in liquid crystal devices taking into account the above characteristics. Despite of bulky end-groups mono-substituted ferrocenomesogens are able to show liquid crystalline properties. As a rule, they exhibit nematic mesomorphism sometimes preceded by smectogenic behavior [4–14]. Introducing asymmetric fragments into the mesogenic core of mono-substituted ferrocenomesogens leads to chiral organization of the mesophases [15–17]. Besides, chiral mesophases can be achieved in multi-substituted ferrocene derivatives with planar chirality. The latter compounds were characterized as weakly ferroelectric liquid crystals [18,19]. Bridged ferrocenes or ferrocenophanes with a minimal structural variation from mono-substituted ferrocenomesogens show enhanced mesomorphism [20,21]. Hexagonal columnar and bicontinuous cubic mesophases were observed in supramolecularly organized ferrocene-containing liquid crystals [22,23] and hexacatenar 1,1′-bis substituted ferrocene derivatives [24]. Recently, unusual mesophases showing ambidextrous chirality were found in unsymmetrically 1,1′-bis substituted ferrocenomesogens, which are preliminarily assigned to mesophases with tetrahedral symmetry [25]. Finally, ferrocene units can be successfully tailored into various liquid crystalline polymer structures [26–31].

The phase transition temperatures in mono-substituted ferrocenes often far exceed 100 °C. Regarding disubstituted liquid crystalline ferrocene derivatives, they often show even higher

* Corresponding author. Department of Physical and Colloid Chemistry, Kazan State Technological University, 68, K. Marks Str., 420015 Kazan, Russia. Tel.: +7 843 2314177; fax: +7 843 2366523.
** Corresponding author. Tel.: +82 2 2123 2645; fax: +82 2 364 7050.
E-mail addresses: oleg.kadkin@bk.ru (O.N. Kadkin), choim@yonsei.ac.kr (M.-G. Choi).

0022-328X/$ – see front matter © 2011 Elsevier B.V. All rights reserved.
doi:10.1016/j.jorganchem.2011.03.013

temperatures of mesophase transitions. It seems there are two major ways for decreasing the temperatures of phase transitions in ferrocene-containing liquid crystals: 1) incorporation of cyclohexane fragments into the rigid core; 2) lowering symmetry of the substituents in the ferrocene unit. The first approach is applicable to both mono- and bis-substituted ferrocenomesogens. T. Hanasaki et al. successfully applied the second approach in some unsymmetrically bis-substituted ferrocenomesogens with the crystal-to-nematic transition below 100 °C [32]. The purpose of the present studies was preparation of various mono-substituted ferrocene-containing liquid crystals with a cyclohexane ring in the rigid core, and investigation of the effect of some selected structural factors on their liquid crystalline properties. In all cases, pure *trans*- isomers of the disubstituted cyclohexanes were used for replacement of benzene rings in the rigid core. In general, a cyclohexane structural unit reduces viscosity and stabilizes the technologically important nematic state [33,34]. Structural variations in the synthesized ferrocenomesogens comprised a different number of carbon atoms in the terminal alkyl chains, the azomethine linking group, the lateral fluoro-substituents, and the 1,3-propylidene bridge in the ferrocene fragment (Scheme 1).

2. Experimental section

2.1. Materials and instruments

Reagent grade chemicals and solvents were purchased from Aldrich (Yongin, Kyounggi-Do, Korea, Korea Branch). Solvents were dried and freshly distilled just before use. Melting points were determined by capillary method in a Stuart Scientific apparatus SMP3. ^{1}H NMR spectra were measured on a Bruker AM 400 with internal TMS standard. Mass-spectra were obtained on a Bruker microflex MALDI-TOF mass spectrometer. Elemental analyses were performed on a Fisons instrument 2A1108 at Korea Institute of Science and Technology. DSC thermographs were obtained on Perkin Elmer Diamond DSC with various scanning rates. Thermo-optical observations were carried out on a Nicon Eclipse E600 Pol optical polarized microscope equipped with a Mettler Toledo FP82 HT hot stage system and Mettler FP90 central processor. Microphotographs were obtained with a Moticam 2300 digital camera. The syntheses of 4-bromophenylferrocene and 4-(4-*n*-decylcyclohexyl)-2,3-difluorobenzene as a mixture of *cis*- and *trans*- isomers are described in our earlier publication [25].

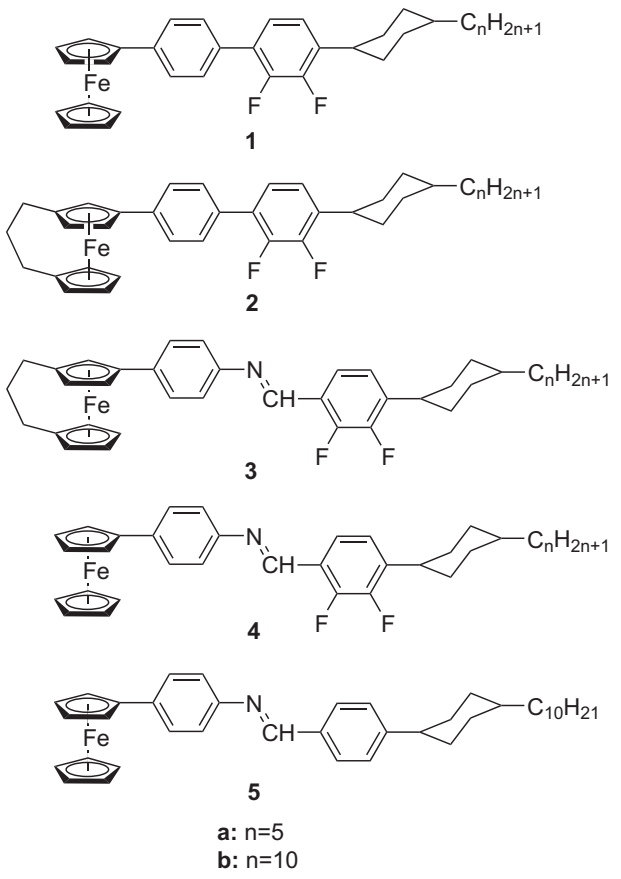

Scheme 1. Chemical structures of the mesogenic ferrocenes **1**–**5** with a cyclohexane fragment in the rigid core.

2.1.1. 4-Bromophenylferrocenophane (***8***)

A mixture of 4-bromoaniline (2.02 g, 11.7 mmol), concentrated H_2SO_4 (7.3 mL, 133 mmol) and water (15 mL) was cooled down to −5 °C and diazotized with a solution of $NaNO_2$ (0.81 g, 11.7 mmol) in water (5 mL). Addition of $NaNO_2$ solution was carried out in such a way so temperature inside of the reaction mixture was not allowed to rise higher than 0 °C. The cold diazonium salt solution was added portion wise to a cold solution (0 °C) of [3]ferrocenophane (1.50 g, 6.6 mmol) in a mixture of diethyl ether (30 mL) and hexadecyltrimethylammonium bromide (0.15 g, 0.4 mmol). The reaction mixture was stirred at 0 °C for 3 h and then at room temperature for overnight. After that the solution was neutralized by NaOH (aq. 10%) and the ether layer was separated with a separation funnel. The aqueous phase was extracted with diethyl ether (×3) then the combined organic extracts were dried over $MgSO_4$, filtered and evaporated under reduced pressure. The residue after evaporation of diethyl ether was placed on an Al_2O_3 column and eluted with hexane. The first fraction containing a mixture of aromatics together with [3]ferrocenophane traces was rejected. The second fraction was collected and evaporated to dryness. The obtained residue was recrystallized from hexane. Yield 1.39 g (58%). Orange powder, m.p. 98.2–99.0 °C; ^{1}H NMR (250 MHz, $CDCl_3$): δ = 7.42–7.22 (m, 5H), 4.47 (d, J = 1.8 Hz, 2H), 4.21 (t, J = 2.1 Hz, 2H), 4.13 (t, J = 1.9 Hz, 1H), 3.96–3.86 (m, 1H), 3.44–3.36 (m, 1H), 2.16–1.83 (m, 6H); MS (EI): 380 (379.99) and Anal. Calcd for $C_{19}H_{17}BrFe$ (%): C 59.88, H 4.50; found: C 59.85, H 4.47.

2.1.2. 4-Aminophenyl ferrocene (***9***)

4-Nitrophenylferrocene (0.40 g, 1.3 mmol) was dissolved in EtOH (5 mL), and 10% Pd/C (0.14 g) was added to the obtained solution. The mixture was reduced in a hydrogenation apparatus under pressure of H_2 (3 atm) for 6 h. The resulting mixture was filtered off through a Celite layer, evaporated to dryness and purified by column chromatography. Yield 0.28 g (78%). Yellowish orange powder, m.p. 152–154 °C (lit. [35] 157–159 °C). ^{1}H NMR (250 MHz, $CDCl_3$): δ = 7.29 (d, J = 8.9 Hz, 2H), 6.64 (d, J = 8.5 Hz, 2H), 4.53 (t, J = 1.8 Hz, 2H), 4.23 (t, J = 1.8 Hz, 2H), 4.03(s, 5H).

2.1.3. 4-(4-n-Pentylcyclohexyl)-2,3-difluorobenzaldehyde (***10a***)

n-Butyllithium (11.8 mL of 2.5 M in cyclohexane, 30.0 mmol) was added dropwise for 30 min to a cooled (−78 °C) solution of 1,2-difluorobenzene (2.74 g, 24.0 mmol) in dry THF (80 mL) under vigorous stirring in dry argon atmosphere. The mixture was stirred at −78 °C for 2.5 h, and then a solution of 4-pentylcyclohexanone (3.66 g, 21.8 mmol) in dry THF (10 mL) was added dropwise at the same temperature for 30 min. The mixture was allowed to warm up to room temperature overnight and the excess of organometallics was quenched with aqueous saturated ammonium chloride (40 mL). The crude product was extracted into ether (×2), and the combined organic layers were dried over anhydrous $MgSO_4$. The obtained solution was filtered, and solvents were evaporated. The residue was

purified on a silica column and the mixture of *cis*- and *trans*- isomers of 4-*n*-pentyl-1-(2,3-difluorophenyl)cyclohexen-2-ol-1 was obtained as a colorless oil (5.78 g, 20.6 mmol, 94%). ^{1}H NMR (250 MHz, $CDCl_3$): δ = 7.42–7.23 (m, 1H), 7.21–6.80 (m, 2H), 2.48–2.28 (m, 2H), 2.12 (s, 1H), 2.00–1.80 (m, 2H), 1.81–1.53 (m, 3H), 1.52–1.11 (m, 11H), 0.89 (t, J = 6.4 Hz, 3H). The obtained mixture of isomers without separation dehydrated by dissolving in THF (60 mL) and slow addition of 95% sulfuric acid (10 mL), and then stirring for 1 h to eliminate OH group. The mixture was quenched in water and extracted into ether (×2). The combined ethereal extracts were washed with saturated $NaHCO_3$ and dried over $MgSO_4$. The obtained solution was filtered and evaporated to dryness. The obtained residue was dissolved in EtOH and hydrogenated to completion in a hydrogenation apparatus in the presence of 10 wt% Pd/C (1.96 g) for 6 h at 3 atm. The crude product was filtered through a Celite layer and ethanol was evaporated. The mixture of *cis*- and *trans*- isomers of 1-(4-*n*-pentylcyclohexyl)-2,3-difluorobenzene was obtained after the purification on a SiO_2 column with hexane as an eluent. Yield 3.69 g (60%), colorless oil. ^{1}H NMR (250 MHz, $CDCl_3$): δ = 7.10–6.88 (m, 3H), 3.03–2.74 (m, 1H), 1.87 (d, J = 9.6 Hz, 2H), 1.80–1.58 (m, 4H), 1.51–1.02 (m, 12H), 0.90 (t, J = 5.6 Hz, 3H). *n*-Butyllithium (6.0 mL of 2.5 M in hexane, 15 mmol) was added dropwise to a stirred and cooled (−78 °C) solution of unseparated isomers of 1-(4-*n*-pentylcyclohexyl)-2,3-difluorobenzene in dry THF under a dry argon pad. The mixture was stirred at −78 °C for 2 h, and then a solution of freshly distilled DMF (0.96 mL, 0.93 g, 12.55 mmol) in absolute THF (10 mL) was added dropwise at −78 °C. The mixture was allowed to warm up to 25 °C over 2 h, quenched with aqueous saturated ammonium chloride (40 mL) and extracted with diethyl ether (×3), and the combined organic layers were dried over anhydrous $MgSO_4$. The obtained solution was filtered, and solvents were evaporated. The residue was purified on a silica column. Yield 2.47 g (39%) of colorless oil as a mixture of *cis*- and *trans*- isomers. Pure *trans*-isomer of 4-(4-*n*-pentylcyclohexyl) benzaldehyde was obtained by multiple recrystallization from pentane. Yield 0.74 g (12%). White crystals, m.p. 66.4–68.8 °C; ^{1}H NMR (400 MHz, $CDCl_3$): δ = 10.29 (s, 1H), 7.60–7.53 (m, 1H), 7.15–7.09 (m, 1H), 2.90 (tt, J_1 = 12.0 Hz, J_2 = 3.4 Hz, 1H), 1.94–1.83 (m, 4H), 1.52–1.43 (m, 2H), 1.37–1.16 (m, 12H), 0.90 (t, J = 7.0 Hz, 3H); MS (EI): 294 (294.18) and Anal. Calcd for $C_{18}H_{24}F_2O$ (%): C 73.44, H 8.22; found: C 73.30, H 8.22.

2.1.4. 4-n-Decylcyclohexyl benzene (**17**) (as a mixture of cis- and trans- isomers)

A mixture of *n*-lauryl aldehyde (14.31 g, 77.7 mmol), methyl vinyl ketone (9.60 mL, 8.06 g, 115.0 mmol) and freshly distilled diethylamine (1.60 mL, 1.13 g, 15.5 mmol) were dissolved in dry THF (100 mL) and then stirred in a high pressure apparatus (autoclave) at 80 °C in argon atmosphere for 50 h. After completion of the reaction an excess of methyl vinyl ketone and THF were evaporated. The crude product was obtained as an oily brown colored solid. A small amount of material (0.10 g) was purified for ^{1}H NMR characterization by SiO_2 column chromatography with toluene/ether (10:1) as an eluent. ^{1}H NMR (250 MHz, $CDCl_3$): δ = 9.55 (d, J = 2.8 Hz, 1H), 2.45 (m, 2H), 2.25 (m, 1H), 2.13 (s, 3H), 1.91–1.72 (m, 2H), 1.71–1.40 (m, 2H), 1.36–1.19 (m, 16H), 0.88 (t, J = 13.7 Hz, 3H). The remaining crude 2-(3-oxobutyl)dodecanal was refluxed with 3 M HCl (200 mL) for 3 h. The product was extracted into ether (×2), the combined ether layers were dried over anhydrous sodium carbonate, filtered and evaporated to dryness. The obtained dark brown liquid was eluted from SiO_2 column with toluene, the eluate was concentrated in a rotary evaporator and decolorized with activated carbon. The remaining toluene was removed under vacuum with heating and stirring (~50 °C) during 3–4 h to give dry 4-*n*-decylcyclohexen-2-one-1 (**15**). Yield 13.62 g (69%), colorless oil. ^{1}H NMR (250 MHz, $CDCl_3$): δ = 6.86 (td, J_1 = 1.3 Hz, J_2 = 2.5 Hz, J_3 = 10.2 Hz, 1H), 5.98 (dd, J_2 = 2.5 Hz, J_3 = 10.2 Hz, 1H), 2.28–2.56 (m, 4H), 2.11 (m, 1H), 1.70 (m, 2H), 1.55–1.14 (m, 16H), 0.89 (t, J = 6.4 Hz, 3H). A solution of *n*-phenyllithium (1.8 M in di-*n*-butylether, 37 mL, 20.5 mmol) was added dropwise during 20 min to a cooled solution (−78 °C) of previously obtained 4-*n*-decylcyclohexen-2-one-1 in dry THF (50 mL) under vigorous stirring in dry argon atmosphere. The mixture was allowed to warm up to room temperature overnight and excess of organometallics were quenched with aqueous saturated ammonium chloride (100 mL). The crude product was extracted into ether (×2), and the combined organic layers were dried over anhydrous $MgSO_4$. The obtained solution was filtered, and solvents were evaporated. The residue was purified on a silica gel column, and 11.15 g (45%) of 4-*n*-decyl-1-phenylcyclohexen-2-ol-1 (**16**) was obtained as a mixture of *cis*- and *trans*- isomers. ^{1}H NMR (250 MHz, $CDCl_3$): δ = 7.85–7.43 (m, 2H), 7.42–7.12 (m, 2H), 6.07–5.88 (m, 1H), 5.85–5.63 (m, 1H), 2.16 (s, 1H), 2.11–1.71 (m, 4H), 1.58–1.09 (m, 18H), 0.88 (t, J = 6.3 Hz, 3H). The obtained material was dissolved in ethanol under dry argon and reduced in a hydrogenation apparatus in the presence of 10% Pd/C (1.60 g) for 6 h at 3 atm. After completion of the reaction the mixture was filtered through a Celite layer and ethanol was evaporated. The residue was purified by SiO_2 column chromatography with hexane as an eluent. Yield 7.66 g (33%), colorless oil. ^{1}H NMR (250 MHz, $CDCl_3$): δ = 7.50–7.09 (m, 5H), 2.68–2.38 (m, 1H), 2.09–1.81 (m, 2H), 1.80–1.57 (m, 4H), 1.51–0.99 (m, 18H), 0.89 (t, J = 6.7 Hz, 3H).

2.1.5. 4-(4-n-Decylcyclohexyl)phenyl bromide (**18**) (as a mixture of cis and trans- isomers)

Bromine (1.20 mL, 23.4 mmol) was added dropwise to a stirred and ice-cooled solution of 4-*n*-decyclohexylbenzene (3.10 g, 10.4 mmol) and I2 (0.03 g, 0.11 mmol) in CH_2Cl_2 (5 mL) in the presence of iron powder (5 g) with the rigorous exclusion of light. After stirring for 1 day at room temperature aq. KOH (10 mL, 20%) was added. The mixture was shaken and extracted with CH_2Cl_2 (×3). Combined extracts were dried over anhydrous Na_2SO_4, filtered and the solvent was evaporated under vacuum. The crude product was purified by silica gel column. Yield 2.09 g (51%). White solid, m.p. 38–41 °C ^{1}H NMR (250 MHz, $CDCl_3$): δ = 7.39 (*trans*) (d, J = 8.4 Hz, 2H), 7.40 (*cis*) (d, J = 8.5 Hz, 2H), 7.08 (*trans*) (d, J = 8.4 Hz, 2H), 7.10 (*cis*) (d, J = 8.8 Hz, 2H), 3.23 (*trans*) (tt, J = 12.2 Hz, J = 3.1 Hz, 1H), 2.52 (m, 1H), 1.86 (d, J = 10.5 Hz, 3H), 1.78–0.98 (m, 20 Hz), 0.88 (t, J = 6.7 Hz, 3H).

2.1.6. 4-(4-n-Decylcyclohexyl)benzaldehyde (**12**)

A solution of n-butyllithium (2.5 M in hexane, 2.50 mL, 6.2 mmol) was added dropwise to a stirred and cooled (−78 °C) solution of 4-(4-*n*-decylcyclohexyl)phenylbromide (**18**) (2.09 g, 5.4 mmol) in dry THF under a dry argon pad. The mixture was stirred at −78 °C for 30 min, and then a solution of freshly distilled DMF (0.38 mL, 0.36 g, 4.9 mmol) in absolute THF (10 mL) was added dropwise at −78 °C. The mixture was allowed to warm up to 25 °C over 2 h, quenched with aqueous saturated ammonium chloride (40 mL) and extracted with diethyl ether (×3). The combined organic layers were dried over anhydrous $MgSO_4$. The obtained solution was filtered, and solvents were evaporated. The residue was purified on a silica column. Yield 0.71 g (40%) of colorless oil as a mixture of *cis*- and *trans*- isomers. The pure *trans* isomer was isolated by multiple recrystallization from pentane. Yield 0.17 g (10%). ^{1}H NMR (250 MHz, $CDCl_3$): δ = 9.97 (s, 1H), 7.80 (d, J = 8.1 Hz, 2H), 7.36 (d, J = 8.0 Hz, 2H) 2.55 (tt, J = 12.2 Hz, J = 2.9 Hz, 1H), 1.90 (d, J = 10.4 Hz, 2H), 1.82–1.00 (m, 22H), 0.88 (t, J = 6.2 Hz, 3H); MS (EI): 328 (328.54) and Anal. Calcd for $C_{23}H_{36}O$ (%): C 84.08, H 11.04; found: C 83.96, H 11.23.

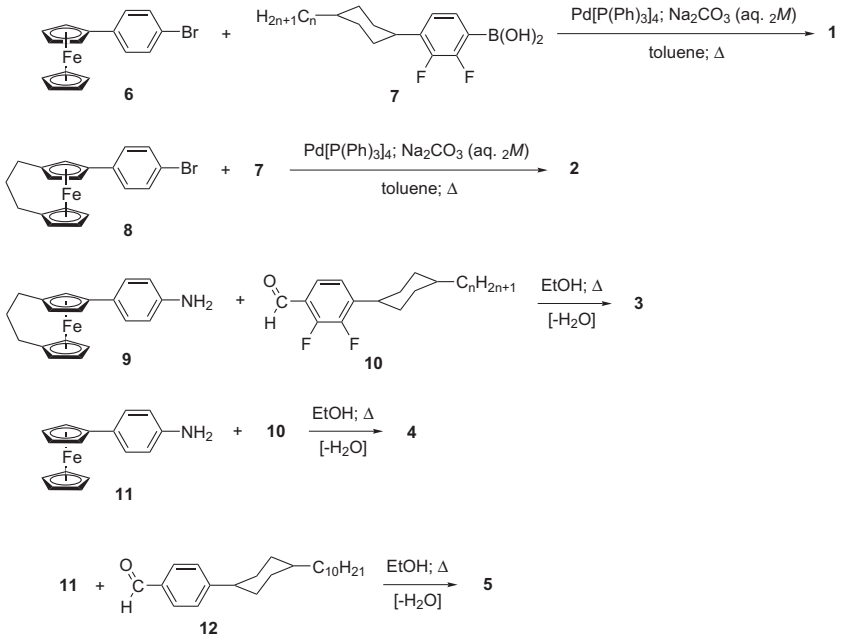

Scheme 2. Synthetic paths to cyclohexane-containing ferrocenomesogens **1**–**5**.

*2.1.7. 4-[4-(trans-4-n-Penthylcyclohexyl)-2,3-difluorophenyl] phenyl ferrocene (**1a**)*

A solution of 4-bromophenylferrocene (0.106 g, 0.31 mmol) was added to a stirred mixture of 4-(trans-4-*n*-penthylcyclohexyl)-2,3-difluorophenylboronic acid (0.115 g, 0.37 mmol), tetrakis-(triphenylphosphine) palladium(0) (0.015 g) in toluene (10 mL) and aqueous sodium carbonate (2.0 M, 2 mL) in argon atmosphere. The stirred reaction mixture was refluxed for 3 days. TLC controlled the reaction completion. The product was extracted into diethyl ether (×2), the ethereal extracts were washed with water and dried over $MgSO_4$. The residue after evaporation of solvents was placed on an Al_2O_3 column, and eluted with hexane. Yield 0.026 g (16%) of orange powder. ^{1}H NMR (250 MHz, $CDCl_3$): $\delta = 7.53$ (d, $J = 8.3$ Hz, 2H), 7.46 (d, $J = 8.2$ Hz, 2H), 7.16 (m, 1H), 7.04 (m, 1H), 4.69 (s, 2H), 4.36 (s, 2H), 4.09 (s, 5H), 2.87 (tt, $J = 12.2$ Hz, $J = 2.9$ Hz, 1H), 1.90 (d, $J = 9.55$ Hz, 2H), 1.82–1.00 (m, 14H), 0.90 (t, $J = 6.6$ Hz, 3H); MS (MALDI-TOF): 526.358 (526.21) and Anal. Calcd for $C_{33}H_{36}F_2Fe$ (%): C 75.28, H 6.89; found: C 74.96, H 7.03.

*2.1.8. 3-{4-[4-(trans-4-n-Penthylcyclohexyl)-2,3-difluorobenzaldimino]phenyl}[3]ferrocenophane (**3a**)*

4-Aminophenyl[3]ferrocenophane (0.050 g, 0.16 mmol) was dissolved in hot ethanol (5 mL) and added to a solution of 4-(4-*n*-penthylcyclohexyl)-2,3-difluorobenzaldehyde (0.046 g, 0.16 mmol) in hot ethanol (5 mL). The reaction mixture was refluxed for 30 min until the formation of orange precipitate. The product was filtered off. Yield 0.0215 g (25%). ^{1}H NMR (250 MHz, $CDCl_3$): $\delta = 8.76$ (s, 1H), 7.94–7.79 (m, 1H), 7.44 (d, $J = 8.37$ Hz, 2H), 7.14 (d, $J = 8.4$ Hz, 2H), 7.07 (t, $J = 7.2$ Hz, 1H), 4.52 (d, $J = 2.2$ Hz, 2H), 4.23 (t, $J = 2.0$ Hz, 2H), 4.14 (t, $J = 1.8$ Hz, 1H), 3.90 (t, $J = 1.7$ Hz, 1H), 3.43 (t, $J = 1.2$ Hz, 1H), 2.88 (tt, $J = 11.9$ Hz, $J = 2.5$ Hz, 1H), 2.26–1.77 (m, 11H), 1.75–1.00 (m, 15H), 0.90 (t, $J = 6.6$ Hz, 3H); MS (MALDI-TOF): 593.507 (593.26) and Anal. Calcd for $C_{37}H_{41}F_2FeN$ (%): C 74.87, H 6.96, N 2.36; found: C 74.68, H 7.03, N 2.40.

3. Results and discussion

3.1. Syntheses

Synthetic routes towards the ferrocene derivatives containing a cyclohexane ring are sketched in Scheme 2. 4-Bromophenyl ferrocene **6** was obtained by applying a Gomberg–Bachman procedure between ferrocene and 4-bromophenyl diazonium salt in the presence of a phase transfer catalyst. Suzuki-Miyaura cross-coupling reaction between **6** and boronic acid **7** yielded compounds **1**(**a**–**b**) (n = **5** or **10**). The same sequence of reactions starting from [3]

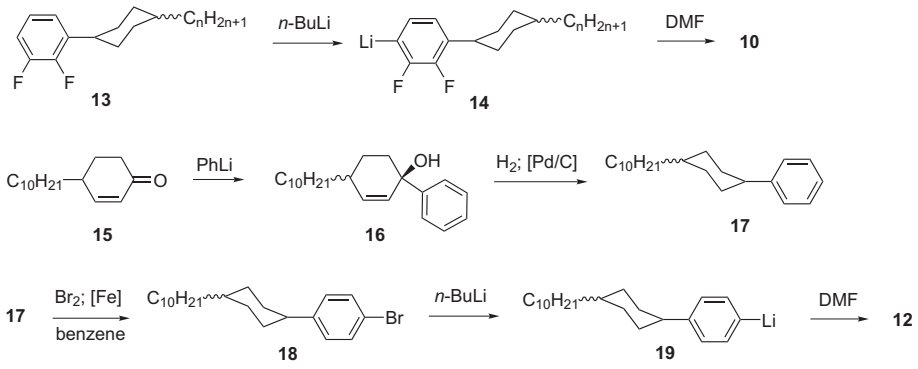

Scheme 3. Synthetic path to cyclohexane-containing aldehydes **10** and **12**.

ferrocenophane [36] led to compounds **2**(**a**–**b**) (n = **5** or **10**). Ferrocene and [3]ferrocenophane derivatives **3**–**5** with the azomethine linkage were obtained by condensation of ferrocene-containing anilines **9** or **11** with cyclohexane-containing aldehydes **10** or **12**.

The synthesis of alkylcyclohexyl-terminated boronic acid **7** and its precursor **13** has been described earlier [25]. Being a valuable intermediate for preparation of boronic acid compound **13** also can be transformed into aldehyde **10** by quenching corresponding organolithium reagent **14** with DMF (Scheme 3). Required *trans*-isomer **10** was isolated from a mixture of isomers by crystallization from hexane, while a *cis*-isomer remains in the mother liquor.

A synthetic path to lithium reagent **19** was less straightforward in comparison with **14**. Contrary to fluorinated aromatic rings, non-fluorinated analogues cannot be lithiated directly. Therefore, it was necessary to prepare a brominated precursor **18** for subsequent lithiation. The cross-coupling reaction of cyclohexenone **15** with phenyllithium allowed obtaining cyclohexenol **16**. Hydrogenation of **16** in the presence of 5% Pd on charcoal under pressure of 3–5 atm led to a mixture of stereoisomers **17**. Ionic bromination of **17** with the powdered iron catalyst afforded p-brominated compound **18**. Lithiation and subsequent quenching of organolithium reagent **19** with DMF finally gave aldehyde **12** as a mixture of *cis*- and *trans*- isomers together with by-products. Required *trans*-isomer **12** crystallizes in hexane.

Elemental analyses, ^{1}H NMR and mass-spectra of the synthesized compounds are in a good agreement with the proposed chemical compositions and structure.

3.2. Thermal behavior

Liquid crystal properties of the synthesized ferrocenomesogens were investigated by means of polarized light microscopy (POM) and differential scanning calorimetry (DSC).

According to POM observations almost all of the compounds **1**–**5** showed the nematic mesophases with characteristic schlieren and marbled textures excluding non-mesomorphic compounds **1** (**a**–**b**). Typical examples of the optical textures are represented in Fig. 1. Appropriate nematic-to-isotropic and isotropic-to-nematic phase transitions were detected on the DSC thermograms as minor peaks (see Supplementary information). In many cases, the obtained compounds showed thermotropic crystal polymorphism.

Compound **1a** is non-mesomorphic but shows a crystal-to-crystal polymorphic transition just before a transition to the isotropic liquid state (see DSC thermograms in Supplementary information). Increasing the length of the terminal alkyl chain in **1b** does not lead to inducing liquid crystallinity as well. Though **1** (**a**–**b**) do not exhibit liquid crystal properties the absence of chemically and hydrolytically unstable groups is exceptionally valuable feature of these compounds. Taking into account their promesogenic architecture, the obtained compounds must be highly adaptable for the mixed liquid crystal compositions.

Earlier investigations of mono-substituted ferrocenomesogens have allowed outlining several structural criteria that are crucial for generating liquid crystallinity and increasing stability of the mesomorphic state [4–14]. Some of those factors are the presence of at least three aromatic rings in the rigid core not counting cyclopentadienyl rings, additional linking groups for widening mesophases and halogen substituents in a lateral position for decreasing transition temperatures. Additionally, all previously studied mono-substituted ferrocenomesogens contained one or several carboxyl, azomethine, azine or azo linking groups. In contrast, compounds **1**(**a**–**b**) include two adjacent benzene rings and one cyclohexane ring in the ferrocene substituent without any linking groups. Normally, a cyclohexane ring in rod-like mesogens can be considered as a part of the rigid core, so the structure **1** can serve as a basic three-ring system for the comparative studies.

The following trends are observed depending on the structural variations from the basic structure **1**. The introduction of the 1,3-propylidene bridge in the ferrocene fragment of compounds **2**(**a**–**b**) leads to appearance of the monotropic nematic mesophases (see Table 1). Thus, the [3]ferrocenophane moiety brings larger geometric anisotropy and closer resemblance to terminal alkyl chains favoring liquid crystalline behavior. Further increase of the geometric anisotropy by addition of the azomethine linking group in compounds (**3a**–**b**) leads to additional enhancement of their liquid crystalline properties in comparison with **2**(**a**–**b**).

Thermal behavior of **3a** is worth a separate consideration. This compound showed an interesting phenomenon of migration of the phase transition points in the subsequent heating cycles. The melting point of the initial crystal form Cr1 in the first heating cycle exceeds by 35 °C the analogous value in the second heating cycle and by 10 °C the isotropization point (see Fig. 2a and b). It should be noted the absence of a crystallization peak in the cooling course and, accordingly, vitrification of the nematic state at room temperature. By all accounts, crystallization in the subsequent heating path occurs into a metastable crystal form Cr2 with the exothermic heat effect. Apparently, the observed Cr2, Cr3 and enantiotropic nematic mesophase in the subsequent heating cycles must be regarded as a metastable with respect to Cr1 from the thermodynamic point of view. In all probability exceptionally high energy barrier for initial

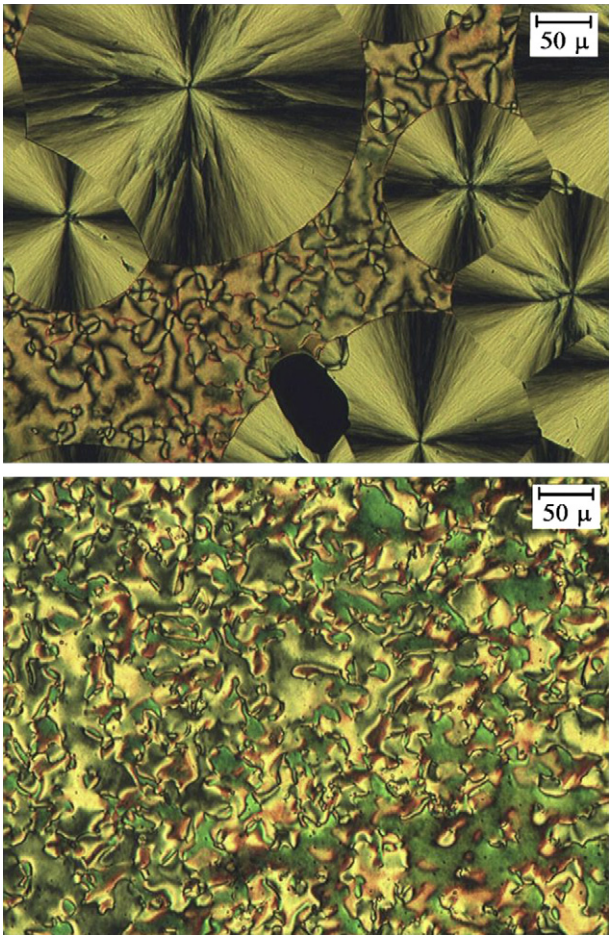

Fig. 1. Microphotographs of a schlieren texture of the nematic mesophase with the growing crystal spherulites obtained at 84 °C on cooling **2a** from the isotropic liquid state (on the top) and a marbled texture of **4b** at 114 °C (on the bottom).

Table 1
Thermal properties of compounds **1**–**5** by DSC and POM.

Compound	Phase transitions[a], oC (ΔH, kJ/mol)			
	1st heating	1st cooling	2nd heating	2nd cooling
1a	Cr[b] 122.6 I (116.8)	I 65.8 Cr (−84.8)	–	–
1b	Cr1 54.1 Cr2 (9.8) Cr1 121.7 I (20.5)	I 112.3 Cr2 (−19.9) Cr2 50.4 Cr1 (−8.9)	–	–
2a	Cr1 139.1 I (21.6)	I [86.4][c] N (−0.1) N 83.0 Cr + G	Cr + G 55.9 Cr2 (−0.9) Cr2 133.0 Cr1 (5.9) Cr1 139.8 I (14.8)	I [86.4] N (−0.1) N 83.0 Cr + G
2b	Cr1 54.0 Cr2 (1.0) Cr2 58.7 Cr3 (5.5) Cr3 124.8 I (32.6)	I[d] [81.8] N (−0.6) N 61.0 Cr3 (−32.2)	Cr3 124.2 (33.7) I	I [82.3] N (−0.7) N 61.3 Cr3 (−31.0)
3a	Cr1 155.3 I (39.7)	I [143.5] N (−0.5)	G 82.0 Cr2 (−7.3) Cr2 121.0 N (27.6) N 144.9 I (0.6)	I [143.6] N (−0.6)
3b	Cr 122.6 I (28.1)	I [116.5] N (−0.3) N 60.8 Cr (−16.7)	Cr 120.3 I (27.5)	I [116.5] N (−0.5) N 61.6 Cr (−18.5)
4a	Cr1 119.2 N (26.2) N 135.2 I (1.3)	I 133.8 N (−1.2) N 63.6 Cr1+Cr2 (−10.0)	G 99.4 Cr (−2.7) Cr1+Cr2119.0N + Cr2 (19.1) N + Cr2 125.0 Cr2 (−24.7) Cr2 142.3 I (26.9)	I 134.0 N (−1.2) N 63.5 Cr1+Cr2 (−10.2)
4b	Cr1 109.6 N (30.2) N 117.1 I (1.2)	I 116.4 N (−1.4) N 81.2 Cr2 (−12.2) Cr2 66.3 Cr3 (−2.3)	Cr3 99.4 (21.1) N N 117.5 I (1.2)	I 116.3 N (−1.3) N 81.1 Cr2 (−11.0) Cr2 65.0 Cr3 (−4.8)
5	Cr 143.4 I (11.2)	I[d] 134.3 N (−0.2) N 126.6 Cr (−14.3)		

[a] Cr – crystal, N – nematic, I – isotropic phases, G – vitrified nematic.
[b] Additionally a crystal polymorphic transition was observed just before isotropisation.
[c] Square brackets are standing for the monotropic phase transitions.
[d] The monotropic phase is detectable with the cooling rate 20 °C/min.

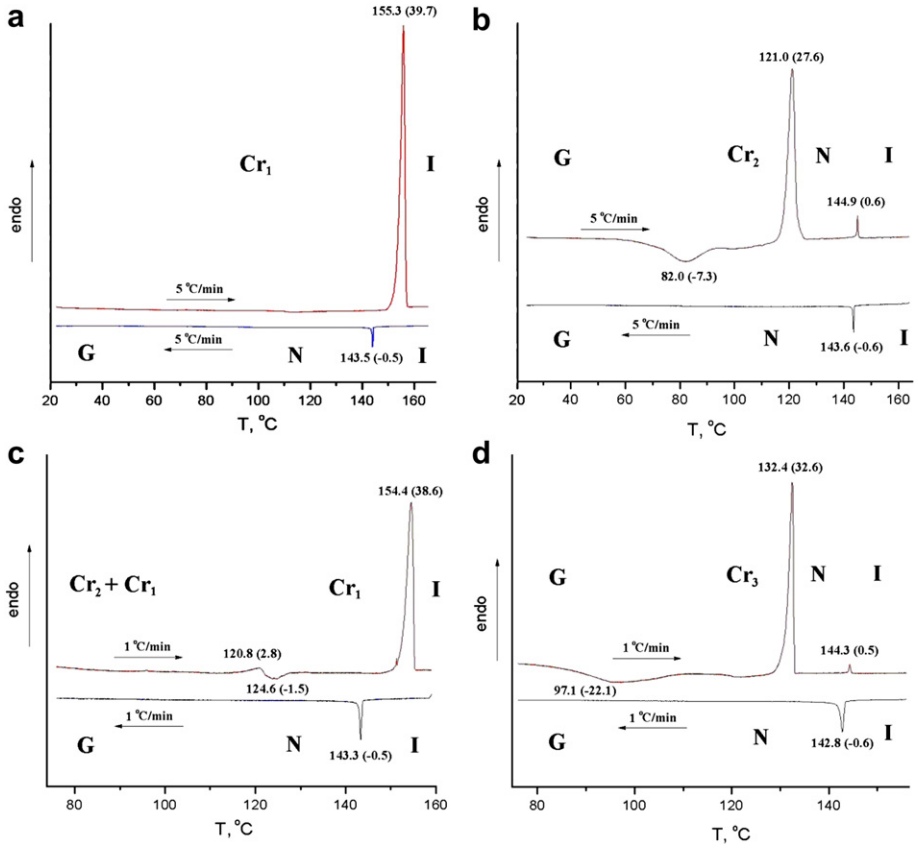

Fig. 2. DSC traces of **3a** (enthalpy values in kJ/mol are given in parentheses): a) the first heating–cooling cycle at 5 °C/min; b) the second heating–cooling cycle at 5 °C/min; c) the same sample after 3 days annealing in the third heating–cooling cycle at 1 °C/min; d) the fourth heating–cooling cycle at 1 °C/min.

nucleation of Cr1 phase from the other crystal polymorphic modifications and nematic liquid leads to slow kinetics of crystallization to the Cr1 form. Even annealing the sample during 2–3 h at 130–135 °C did not lead to appearance of the stable crystal modification Cr1. Nevertheless, the system returns to an initial state by keeping the nematic glass at room temperature for several days (Fig. 2c). Changing the scanning rate from 5 °C/min to 1 °C/min revealed the existence of another metastable crystal form Cr3 with the melting point exceeding by 10 °C the previous metastable form Cr2 (Fig. 2d). Moreover, even at this slow heating rate compound **3a** shows enantiotropic mesomorphism contrary to its initial monotropic behavior. The sharpness of the appropriate DSC peaks undoubtedly indicates the presence of the above crystal forms Cr2 and Cr3 as individual modifications but not the mixtures. Complicated thermal behavior of ferrocenyl compounds with multiple melting points is not uncommon [37]. It is noteworthy that the analogous compound **3b** with a longer terminal alkyl chain shows the regular monotropic nematic mesophase in repeated DSC cycles (see Supplementary information).

Compounds **4**(**a**–**b**) without the 1,3-propylidene bridge exhibited enantiotropic nematic mesomorphism contrary to **3**(**a**–**b**) showing metastable mesophases. Normally ferrocenophane derivatives displayed better mesophase characteristics with reference to analogous derivatives of the unbridged ferrocene [20,21]. A positive effect of the 1,3-proppylidene bridge in the reported cases was connected with lowering the mesophase transitions and broadening mesophases. In the present case [3]ferrocenophane derivatives **3** (**a**–**b**) have higher melting points in comparison with ferrocene derivatives **4**(**a**–**b**) and comparable clearing points. The latter parameter characterizes thermal stability of the nematic phase. It looks like the higher melting points are the main motive for the comparatively poor mesomorphism of **3**(**a**–**b**) in spite of their larger geometric anisotropies and resemblance of the 1,3-propylidene bridge to alkyl substituents. On the other hand, ferrocenophane derivatives as alkylidene terminated mesogens follow in this case a well-known rule for homologous series of liquid crystals with the mesophase transition temperatures below 120 °C, when the longer alkyl chains increase the phase transition temperatures.

Both compounds **4**(**a**–**b**) also show crystal polymorphism and migration of the melting points in subsequent heating cycles. Compound **4a** exhibited the enantiotropic nematic mesophase as it can be seen from its DSC thermogram at the scanning rate of 5 °C/min (Fig. 3a). Unexpectedly, on the second heating–cooling cycle the transition to the nematic state was immediately followed by exothermic crystallization of the sample (Fig. 3b). Apparently, the latter crystal form Cr2 is thermodynamically more stable than the initial Cr1 and the nematic states observed in the first heating cycle. It is noteworthy that the nematic-to-isotropic transition is absent in the second DSC cycle and replaced by a large crystal-to-isotropic peak. The melting point of the Cr2 phase exceeds by 7 °C the nematic-to-isotropic liquid phase transition in the first heating cycle. Obviously, the crystal form Cr2 was not observed in the first heating cycle due to the slow kinetics of the crystallization process. We suggest that the initial crystal form Cr1 is present in the virgin sample. The formation of the second crystal form Cr2 from the nematic state in this case must be extremely slow in the absence of crystal seeds. However, both crystal forms may be present in the sample after cooling from the isotropic liquid state. So, the second heating process leads to the melting of the Cr1 phase to the nematic state which immediately crystallizes to the stable Cr2 state in the presence of unmelted Cr2 centers. In fact, DSC measurements at 1 °C/min allowed detecting the Cr2 phase even in the first heating–cooling cycle (Fig. 3c). Moreover, the transition Cr1-to-Cr2 in the latter case is hidden and occurs with a negligible heat effect. Thus, we observe in **4a** a delicate thermodynamic balance between

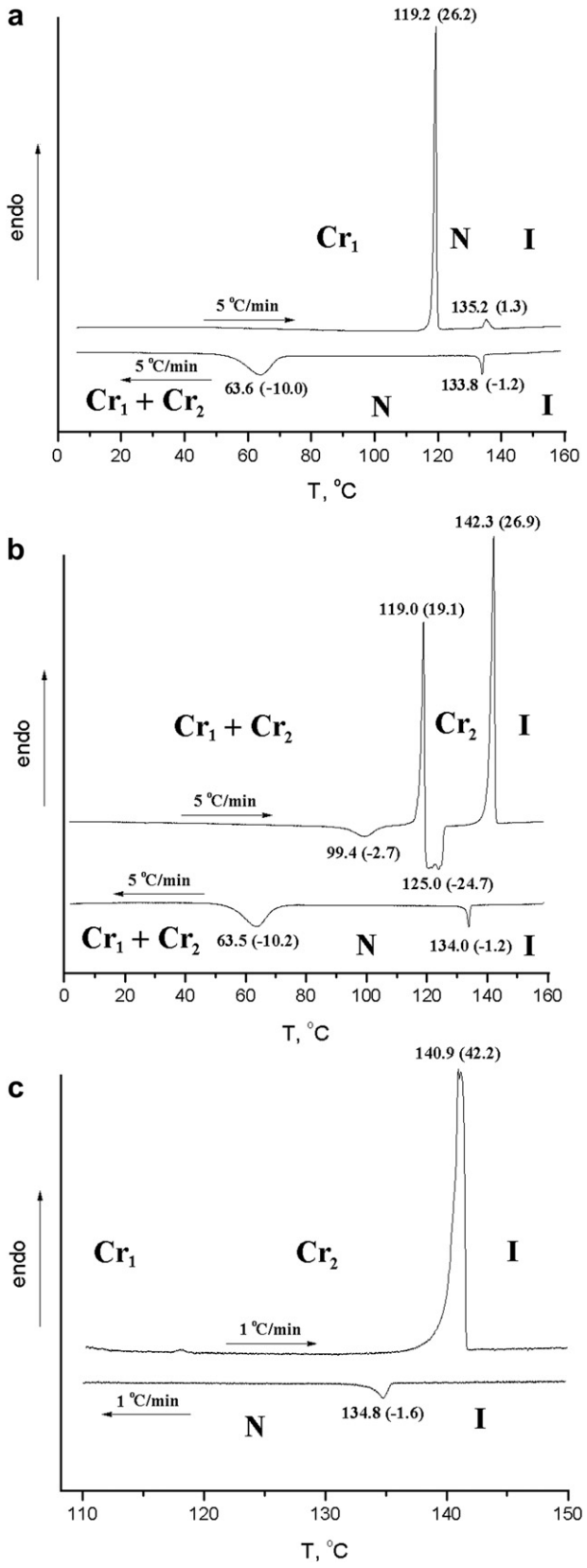

Fig. 3. DSC traces of **4a** (enthalpy values in kJ/mol are given in parentheses): a) the first heating–cooling cycle at 5 °C/min; b) the second heating–cooling cycle at 5 °C/min; c) the first heating–cooling cycle at 1 °C/min in the range of 110–150 °C.

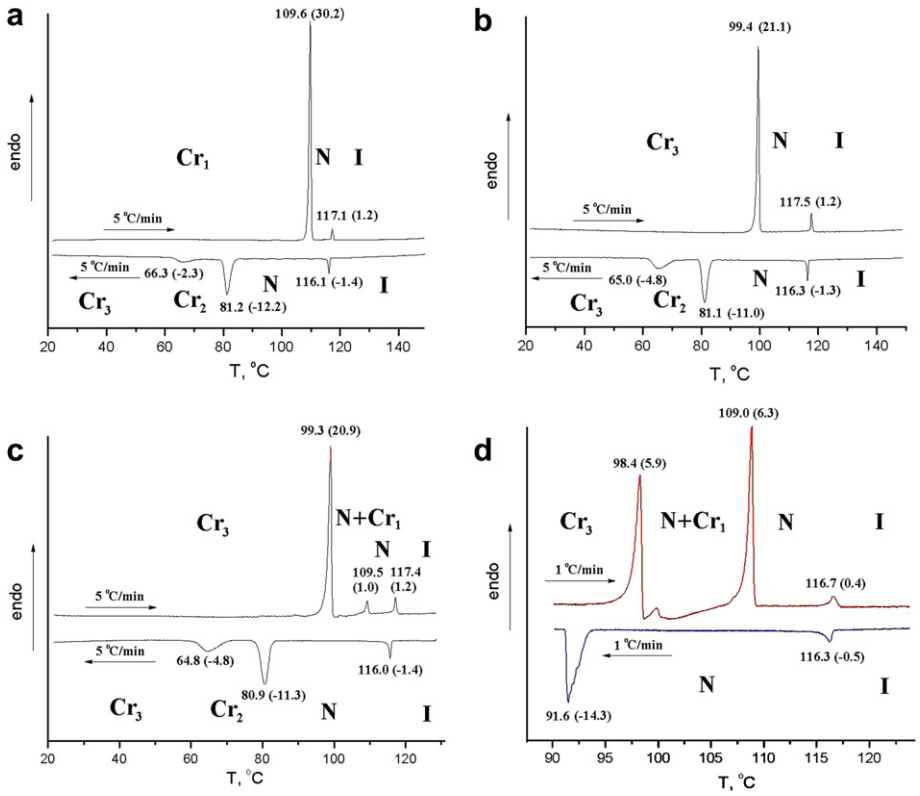

Fig. 4. DSC traces of **4b** (enthalpy values in kJ/mol are given in parentheses): a) the first heating–cooling cycle at 5 °C/min; b) the second heating–cooling cycle at 5 °C/min; c) the third heating–cooling cycle at 5 °C/min after annealing the sample at room temperature for 3 days; d) the fourth heating–cooling cycle at 1 °C/min in the range of 90–130 °C.

stable and metastable crystal forms, which leads in due order to the rate-depended alteration between enantiotropic and monotropic nematic mesomorphism.

Compound **4b** with the longer terminal alkyl substituent also shows complex behavior connected with the crystal polymorphism. The enantiotropic nematic mesophase was observed by POM and the corresponding phase transitions are measured by DSC at the scanning rate of 5 °C/min (Fig. 4a). A significant drop approximately by 10 °C down was detected for the crystal-to-nematic transition in the second heating–cooling cycle (Fig. 4b). It appears that the crystal form Cr1 of **4b** obtained on crystallization from the solvent is not formed on crystallization from the isotropic melt. The enthalpy of the crystal-to-nematic transition in the second DSC cycle is significantly lower than in the first heating course (see Table 1). Consequently, during crystallization from the nematic melt the metastable crystal phases Cr2 and Cr3 with higher energy were obtained. And a transition of the latter Cr3 phase to the thermodynamically stable Cr1 state is again prevented by slow kinetics of the crystallization processes. However, after annealing the sample at room temperature for several days a small peak of the Cr1-to-nematic transition appears in a DSC thermogram at the scanning rate 5 oC/min (Fig. 4c). The slower scanning rate of 1 °C/min revealed exothermic crystallization processes after a Cr3-to-nematic peak at 99 °C and an increased peak of the Cr1-to-nematic transition at 109 °C (Fig. 4d).

A comparison of **5** with **4b** clearly demonstrates a positive role of lateral fluorination in the pursuance of low-temperature ferrocene-containing nematics. The latter fact has been already emphasized in systematic investigations of Loubser and Imrie [14]. Dissimilar to fluorinated **4b** showing enantiotropic mesomorphism its non-fluorinated counterpart **5** exhibits only the monotropic nematic phase. The considerably higher melting point of **5** could be a reasonable explanation of its poor mesomorphism.

Thus, a remarkable drift of the melting points was observed in compounds **3a** and **4**(**a**–**b**). According to DSC experiments the presence of metastable crystal forms and extremely slow kinetics of transition to the stable crystal states have been recognized as being responsible for this unusual behavior.

4. Conclusions

A series of novel mono-substituted ferrocenomesogens with a cyclohexane ring incorporated in the rigid core has been investigated by using DSC and thermal polarisational microscopy. A basic structure with two aromatic and one carbocyclic ring in the ferrocene substituent does not exhibit liquid crystallinity. The addition of the 1,3-propylidene bridge in the ferrocene moiety led to appearance of the monotropic nematic mesophase. Inclusion of the azomethine linkage group into the rigid core significantly enhances liquid crystallinity and results in the enantiotropic nematic mesophase. Lateral fluoro-substituents in the benzene rings play a positive role in lowering transition temperatures and stabilizing the nematic state. Migration of the phase transition points was observed in some of the synthesized compounds. A delicate thermodynamic balance between the metastable and stable crystal forms leads to alteration between enantiotropic and monotropic mesomorphism depending on the thermal prehistory of the sample. Chemically resistant, low-viscous and low-temperature ferrocene-containing liquid crystals potentially can be used as individual compounds or as mixtures in various technological applications.

Acknowledgements

This work has been supported by a grant from the Korea Science and Engineering Foundation (KOSEF) through the Center for

Bioactive Molecular Hybrids (CBMH) and the program Brain Korea 21 (BK-21).

Appendix A. Supplementary material

Supplementary data related to this article can be found online at doi:10.1016/j.jorganchem.2011.03.013.

References

[1] A.M. Giroud-Godquin, Coord. Chem. Rev. 178–180 (1998) 1485–1499.
[2] R. Gimenez, D.P. Lydon, J.L. Serrano, Curr. Opin. Solid State Mater Sci. 6 (2002) 527–535.
[3] B. Donnio, D. Guillon, D.W. Bruce, R. Deschenaux, Metallomesogens (Vol. ed.: D. O'Hare). in: R.H. Crabtree, D.M.P. Mingos (Eds.), Comprehensive Organometallic Chemistry III: From Fundamentals to Applications, Applications III: Functional Materials, Environmental and Biological Applications, vol. 12. Elsevier, Oxford, UK, 2006, pp. 195–294 Chapter 12.05.
[4] C. Imrie, P. Engelbrecht, C. Loubser, C.W. McCleland, Appl. Organomet. Chem. 15 (2001) 1–15.
[5] I. Cârlescu, A.M. Scutaru, D. Apreutesei, V. Alupei, D. Scutaru, Liq. Cryst. 34 (2007) 775–785.
[6] I. Cârlescu, A.M. Scutaru, D. Apreutesei, V. Alupei, D. Scutaru, Appl. Organomet. Chem. 21 (2007) 661–669.
[7] N. Nakamura, T. Nio, T. Okabe, Mol. Cryst. Liq. Cryst. 460 (2006) 85–92.
[8] W.-C. Shen, Y.-J. Wang, K.-L. Cheng, G.-H. Lee, C.-K. Lai, Tetrahedron 62 (2006) 8035–8044.
[9] D. Apreutesei, G. Lisa, D. Scutaru, N. Hurduc, J. Optoelectron. Adv. M. 8 (2006) 737–740.
[10] M.V. Makarov, L.N. Kuleshova, D.W.M. Hofmann, V.P. Dyadchenko, M. Yu, Crystallogr. Rep. 51 (2006) 792–803.
[11] M.V. Makarov, D.A. Lemenovskii, A.E. Bruce, M.R.M. Bruce, V.P. Dyadchenko, Liq. Cryst. 33 (2006) 485–494.
[12] C. Imrie, C. Loubser, P. Engelbrecht, C.W. McCleland, Y. Zheng, J. Organomet. Chem. 665 (2003) 48–64.
[13] C. Imrie, P. Engelbrecht, C. Loubser, C.W. McCleland, V.O. Nyamori, R. Bogardi, D.C. Levendis, N. Tolom, J. van Rooyen, N. Williams, J. Organomet. Chem. 645 (2002) 65–81.
[14] C. Loubser, C. Imrie, J. Chem. Soc. Perkin Trans. 2 (1997) 399–409.
[15] D. Apreutesei, G.H. Mehl, D. Scutaru, Liq. Cryst. 34 (2007) 819–831.
[16] T. Seshadri, H.-J. Haupt, U. Flörke, G. Henkel, Liq. Cryst. 34 (2007) 33–47.
[17] D. Apreutesei, G. Lisa, H. Akutsu, N. Hurduc, S. Nakatsuji, D. Scutaru, Appl. Organomet. Chem. 19 (2005) 1022–1037.
[18] T. Chuard, S.J. Cowling, M. Fernandez-Ciurleo, I. Jauslin, J.W. Goodby, R. Deschenaux, Chem. Commun. (2000) 2109–2110.
[19] J. Brettar, T. Bürgi, B. Donnio, D. Guillon, R. Klappert, T. Scharf, R. Deschenaux, Adv. Funct. Mater. 16 (2006) 260–267.
[20] A. Werner, W. Friedrichsen, J. Chem. Soc. Chem. Commun. (1994) 365–366.
[21] O. Kadkin, H. Han, Yu. Galyametdinov, J. Organomet. Chem. 692 (2007) 5571–5582.
[22] P. Massiot, M. Impéror-Clerc, M. Veber, R. Deschenaux, Chem. Mater. 17 (2005) 1946–1951.
[23] R. Deschenaux, F. Monnet, E. Serrano, F. Turpin, Helv. Chim. Acta 81 (1998) 2072–2077.
[24] J.-S. Seo, Y.-S. Yoo, M.-G. Choi, J. Mater. Chem. 11 (2001) 1332–1338.
[25] O.N. Kadkin, E.H. Kim, Y.J. Rha, S.Y. Kim, J. Tae, M.-G. Choi, Chem. Eur. J. 15 (2009) 10343–10347.
[26] P. Singh, M.D. Rausch, R.W. Lenz, Polym. Bull. 22 (1989) 247–252.
[27] X.-H. Liu, D.W. Bruce, I. Manners, J. Organomet. Chem. 548 (1997) 39–56.
[28] R. Deschenaux, F. Turpin, D. Guillon, Macromolecules 30 (1997) 3759–3765.
[29] R. Deschenaux, I. Jauslin, U. Scholten, F. Turpin, D. Guillon, B. Heinrich, Macromolecules 31 (1998) 5647–5654.
[30] S. Senthil, P. Kannan, J. Polym. Sci. A: Polym. Chem. 40 (2002) 2256–2263.
[31] P. Kannan, S. Senthil, R. Vijayakumar, R. Marimuthu, J. Appl. Polym. Sci. 86 (2002) 3494–3501.
[32] T. Hanasaki, K. Matsushita, T. Watanabe, S. Enomoto, Y. Sato, Mol. Cryst. Liq. Cryst. 351 (2000) 103–110.
[33] P. Kirsch, M. Bremer, Angew. Chem. Int. Ed. 39 (2000) 4216–4235.
[34] S. Singh, D.A. Dunmur, Nematic liquid crystals. in: S. Singh, D.A. Dunmur (Eds.), Liquid Crystals: Fundamentals. World Scientific, Singapore, 2002, pp. 92–173.
[35] W.F. Little, A.K. Clark, J. Org. Chem. 25 (1960) 1979–1982.
[36] T.D. Turbitt, W.E. Watts, J. Organomet. Chem. 46 (1972) 109–117.
[37] T. Hanasaki, M. Ueda, N. Nakamura, Mol. Cryst. Liq. Cryst. 237 (1993) 329–336.